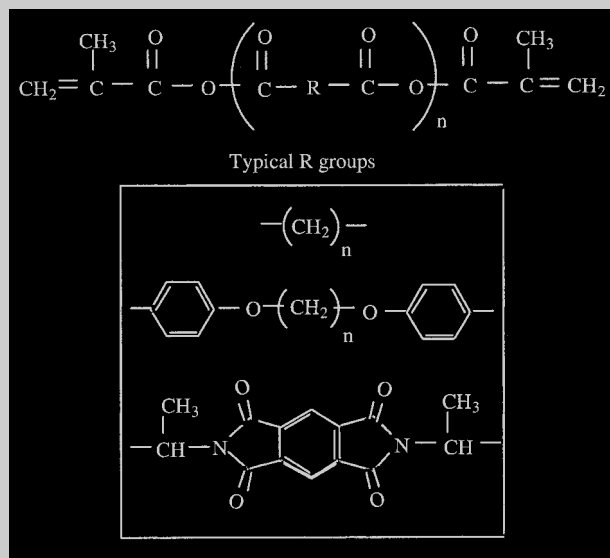


Feature Article: The synthesis of multifunctional monomers that can be photopolymerized to form highly cross-linked, surface degrading polymers is reviewed. Typical reaction behavior of multifunctional monomers is discussed, as well as the difficulties associated with photopolymerizing thicker materials and the benefits of temporal control of the photoinitiation process. Characterization of the degradation behavior of these networks indicates a surface erosion mechanism where the rate of degradation is readily controlled to produce materials that degrade on time scales of days to months. To provide insight into the structural evolution during the polymerization of multifunctional monomers, the degradation products, specifically the kinetic chain lengths, have been analyzed using MALDI-TOF spectroscopy. Additionally, the use of photopolymerizable, degrading polymers for drug delivery is illustrated, and other potential applications of these unique polymers are mentioned.

General structure of methacrylated anhydride monomers.



Polymerizations of Multifunctional Anhydride Monomers to Form Highly Crosslinked Degradable Networks

Kristi S. Anseth,^{*1,2} Deborah J. Quick¹

¹ Department of Chemical Engineering, University of Colorado, Campus Box 424, ECCH 111, Boulder, CO 80309, U.S.A.
Fax: 001-303-492-4341; E-mail: kristi.anseth@colorado.edu

² Howard Hughes Medical Institute, University of Colorado, Boulder, CO 80309, U.S.A.

Introduction

Photopolymerization of multifunctional monomers allows for the facile production of highly crosslinked polymer networks that are useful in a variety of applications. Polymer networks with a high crosslinking density have increased thermal stability, mechanical strength, and resistance to solvent absorption. In addition, photoinitiated polymerization of multifunctional monomers occurs rapidly (e.g., seconds to minutes) with temporal and spatial control of the reaction. The useful properties of the final polymer networks along with the advantages of photofabrication processes have led to increased demand and new applications for these materials. For example, photopolymerizations of multifunctional monomers are used in numerous industries to produce a variety of products including dental restorative materials, coatings for optical fibers, contact lenses, and flexible printing plates.^[1–4]

While the applications for photopolymerization processes are expanding, understanding the complex reactions of multifunctional monomers and how the reaction conditions couple to the densely crosslinked network structure and final material properties is difficult. Specifically, dramatic changes occur in the species mobility as the liquid monomer is rapidly converted to a glassy (or rubbery) solid network. Diffusion limitations lead to reaction behavior typified by autoacceleration and deceleration,^[5–8] trapping of radicals,^[9,10] limited double bond conversion,^[11,12] unequal reactivity of functional groups,^[13–15] microstructural heterogeneity,^[16,17] and volume relaxation effects.^[18] The insolubility of the evolving network structure further complicates and limits experimental techniques to characterize the structural evolution and reaction behavior. However, understanding the complex relationships between the reaction condi-

tions, network structure, and final material properties is critically important since many applications of photopolymerized materials require a fully functional product upon fabrication (e.g., dental restorations). To this end, numerous groups^[9, 19–22] are developing advanced experimental techniques and models to improve upon our current understanding of multifunctional monomer polymerizations.

Our research group has been particularly interested in the development of multifunctional monomers that can be photocrosslinked to form degradable networks. The motivation for this work was two-fold. First, using biocompatible initiation conditions, photopolymerization provides a technique whereby polymers can be synthesized in the body under physiological conditions, and multifunctional monomers that react to form degradable polymer networks are particularly beneficial for many medical applications as in situ forming biomaterials (e.g., drug delivery, fracture fixation, tissue sealants). Hubbell and others^[23–26] pioneered some of the first efforts in designing photopolymerizable, functionalized macromers that react to form degradable hydrogel networks for applications to prevent post-surgical adhesions. Our group was interested in synthesizing a series of multifunctional monomers that could be photopolymerized to form highly crosslinked, high-strength polymers that

would resist water penetration and thereby degrade with a surface controlled mechanism. Secondly, since the final networks are degradable, analyzing the degradation products can provide further insight related to the fundamental characterization of multifunctional monomer polymerizations and the influence of reaction conditions on the evolution of crosslinked network structure. Specifically, a unique opportunity exists to obtain direct experimental information related to the distribution of kinetic chain lengths in highly crosslinked networks and further insight related to the initiation, propagation, termination, and chain transfer mechanisms during multifunctional monomer polymerizations.

This manuscript reviews a class of multifunctional anhydride monomers that can be photopolymerized to form surface eroding networks. From a biomaterials perspective, these networks provide advantages over the commonly used poly(lactic acid) (PLA) and poly(glycolic acid) (PGA) based systems. PLA, PGA, and their copolymer degrade via a bulk mechanism which can lead to an early loss in mechanical properties and a burst of acid products at the late stages of degradation. Surface eroding polymers circumvent these problems and can be especially beneficial for drug delivery and load bearing medical applications. In addition, systems that can be polymerized in situ provide benefits over materials that must



Kristi S. Anseth received her B.S. in Chemical Engineering from Purdue University in 1992 and her Ph.D. in Chemical Engineering from the University of Colorado in 1994. Upon completion of her Ph.D., Dr. Anseth was an NIH Postdoctoral Fellow at the Massachusetts Institute of Technology and subsequently accepted a faculty position at the University of Colorado in 1996. Dr. Anseth is presently a Howard Hughes Medical Institute Assistant Investigator and the Patten Associate Professor of Chemical Engineering at the University of Colorado, and her research interests involve the application of photopolymerization technology to the development of degradable polymers for medical and biological applications. Her research program has been recognized and awarded an NSF CAREER Award, NIH FIRST Award, a Packard Foundation Fellowship, and the MRS Outstanding Young Investigator Award. Dr. Anseth is also a dedicated teacher, who has received the Department's Outstanding Graduate Teaching Award in 1997, the College of Engineering's Peebles Teaching Innovation Award in 1998, the ASEE Rocky Mountain Section Dow Outstanding New Faculty Award in 1999, a Camille Dreyfus Teacher-Scholar Award in 2000, and the Boulder Faculty Assembly Teaching Excellence Award in 2000.



Deborah J. Quick received her Bachelor's degree in chemical engineering with a bio-sciences option in 1993 from North Carolina State University. Her undergraduate study was supported by an NSF Corporation Scholarship. She attended graduate school at Cornell University with the support of a Fred T. Rhodes Fellowship and completed her Master's degree in 1995. After obtaining her MS degree, she worked for 3 years at SmithKline Beecham in King of Prussia, PA in a process development group optimizing protein production by CHO cells. She is currently a graduate student pursuing a Ph.D. degree under the supervision of Dr. Kristi S. Anseth in the Department of Chemical Engineering at the University of Colorado in Boulder. Her project is developing a method for delivering DNA from photopolymerizable, degradable polymers. She is supported by a Department of Education fellowship for Graduate Assistance in Areas of National Need (GAANN).

be fabricated *ex vivo*. The following sections discuss the major advantages and challenges in developing and characterizing photocrosslinkable and degradable monomer systems, particularly with respect to their application as biomaterials.

Results and Discussion

Multifunctional Monomer Chemistry

Methacrylated monomers of varied hydrophobicity and functionality have been synthesized from multi-acids with methacrylic anhydride.^[27, 28] The adaptability of this synthesis allows for a wide range of possible monomer structures, as shown in Figure 1, and a correspondingly diverse array of resulting polymer properties. For example, the presented dimethacrylated monomers react to form networks with different degradation rates (a few days to several months), mechanics (rubbery to glassy), and polymerization behavior (radical trapping, onset of autoacceleration, and time to complete reaction). If one increases the functionality of the monomer by using a triacid, such as citric acid, significant increases in the crosslinking density can result accompanied by an increase in the polymerization rate and final modulus of the network.

The backbone chemistry of the monomers is easily modified to incorporate a wide range of substituents, from hydrophobic aromatic groups to rigid imide units, as seen with methacrylated 1,6-bis(carboxyphenoxy)hexane and methacrylated pyromellitylimidoalanine, respectively. The backbone chemistry of the monomer has a significant impact on the resulting crosslinked network's degradation and mechanical properties. Specifically, the hydrophobicity of the backbone chemistry controls the rate of degradation, and networks based on MCPH degrade two orders of magnitude more slowly than networks based on MSA. Interestingly, the molecular weight of the monomers, which is controlled by the size of the diacid and the degree of oligomerization, dominates the final network structure and mechanics, so the degradation rate and mechanical behavior are readily decoupled. The incorporation of stiff, imide groups into the backbone of

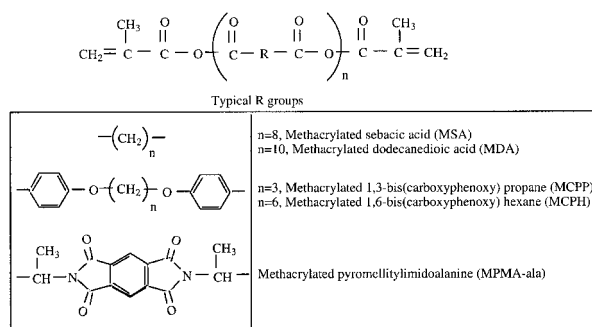


Figure 1. General structure of methacrylated anhydride monomers.

the anhydride monomers by functionalized amino acids increases mechanical and thermal stability without significantly altering the rate and mode of degradation.^[29] While the number of different amino acids (naturally occurring or otherwise) is immense, the resulting combination of imide containing monomer structures is equally diverse, and furthermore, functionalized biosequences may be added to promote targeted biological responses.

Typical Reaction Behavior of Multifunctional Monomers

Figure 2 contains a characteristic reaction rate profile for a multifunctional monomer that exhibits many classical complexities of diffusion controlled polymerizations.^[30] In this figure, the rate of polymerization is plotted as a function of conversion for two photoinitiated polymerizations of diethylene glycol dimethacrylate (DEGDMA), and several features are noteworthy. From the onset of the reaction, the polymerization rate increases with conversion, which has generally been referred to as autoacceleration. During this portion of the polymerization, the mobility of the radicals is decreasing dramatically which leads to a reduced termination rate. The decreased rate of termination leads to a large build-up in the radical concentration, thus increasing the polymerization rate. It should be noted, as has been shown elsewhere,^[31] that at some point during autoacceleration, the termination mechanism becomes reaction diffusion controlled. Instead of termination occurring by segmental diffusion of radicals, the radicals are mobile primarily by reacting through unreacted double bonds present in the system. The polymerization reaction then reaches a maximum rate and begins to decrease. This region has generally been referred to as autodeceleration, where vitrification and crosslinking restrict and eventually stop the propagation reaction. During this phase of the reaction, the rate of termination continues to decrease; however, the restriction of propagation dominates the decreasing rate.

Furthermore, a maximum double bond conversion is reached that is less than 1, and this maximum attainable

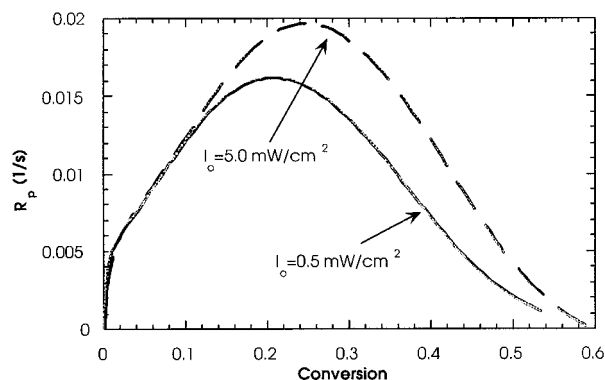


Figure 2. Polymerization rate as a function of conversion for DEGDMA at two different light intensities: 5.0 mW/cm² (---) and 0.5 mW/cm² (—).

conversion increases for systems that are polymerized at a faster rate. This increased double bond conversion is likely related to the delay in volume shrinkage rate, which leads to an increased free volume and increased mobility in polymerizations which proceed at faster rates (i.e., those initiated by higher light intensities or higher initiator concentrations). Further evidence of this volume relaxation effect is apparent by observing the asymmetry of the two curves, which is most easily observed as the polymerizations reach their maximum rate. The lower rate polymerization reaches a maximum rate at 20% conversion while the higher rate polymerization reaches a maximum rate at 25% conversion. In general, the curve at higher rates is shifted to higher conversions because of the delay in volume shrinkage. The asymmetry in these curves indicates that the kinetic constants for polymerization are functions of the double bond conversion, as well as the rate at which that double bond conversion is reached.

These complexities in the reaction behavior of multifunctional monomers have many significant implications on the final structure of the resulting network. For example, trapped radicals will exist in the highly crosslinked network. Pendant double bonds will have a different reactivity than monomeric double bonds due to the proximity of the pendant group to the locally propagating radical. In general, this proximity leads to enhanced reactivity of the pendant double bond at low conversion and the formation of highly crosslinked and cycled microgel regions. Later in the polymerization at much higher conversion, pendant groups can become shielded and the relative reactivity of monomeric to pendant double bonds increases. This changing reactivity has important structural implications and also impacts the amount of unreacted monomer that exists when the maximum double bond conversion is reached.

Reaction Behavior of Multifunctional Monomers that Form Degradable Networks

Differential scanning photocalorimetry and infrared spectroscopy were used to characterize the polymerization behavior, curing time, and maximum double bond conversion of dimethacrylated anhydride monomers.^[32] Typical results are presented for MSA polymerized under simulated physiological conditions (i.e., in air at 37 °C). The results are presented in Figure 3 and illustrate how the rate of initiation, as controlled by the light intensity and initiator concentration, can be used to alter the conversion, polymerization rate, and total polymerization time. In general, the rate curves exhibit characteristics typical of non-degrading multifunctional monomer polymerizations that were discussed above. An early onset of autoacceleration, leading to a dramatic increase in the polymerization rate, is followed by a marked autodeceleration. The majority of the double bonds are consumed within the first minute or two (depending on the initiating conditions), after which the polymerization rate becomes

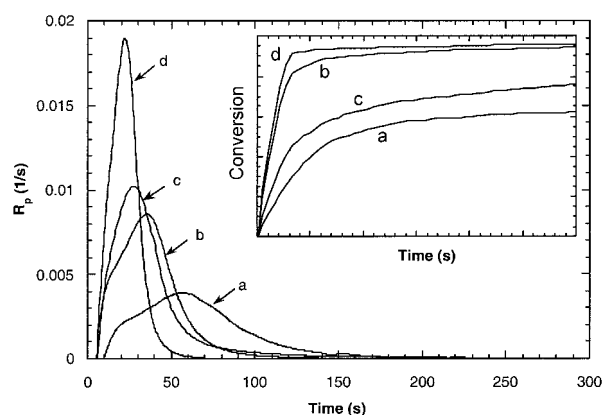


Figure 3. Effect of light intensity and initiator concentration on the rate of polymerization and double bond conversion (inset) of MSA: (a) 0.1 wt.-% DMPA, 5 mW/cm², (b) 1.0 wt.-% DMPA, 5 mW/cm², (c) 0.1 wt.-% DMPA, 150 mW/cm², (d) 1.0 wt.-% DMPA, 150 mW/cm².

vanishingly small. The autoacceleration peak becomes more pronounced as higher initiation rates are used. While the effects of the initiator concentration and light intensity on the polymerization rate follow expected trends, the results are complicated by volume relaxation. In addition, the rate of polymerization, R_p , does not scale with the rate of initiation, R_i , to the one-half power as predicted by classical chain polymerization kinetics with bimolecular termination. Instead, a much lower dependence is experimentally observed, which others have seen during the polymerization of multifunctional methacrylate.^[30]

FT-IR results further characterize the polymerization behavior and quantify the maximum attainable double bond conversion. These results illustrate the ability to control the polymerization time through simple changes in the initiation rate. For example, MSA is polymerized in 30 s when exposed to 150 mW/cm² of UV light and 1.0 wt.-% initiator, whereas >200 s are required when the initiator concentration is decreased an order of magnitude to 0.1 wt.-%. The time of polymerization is important for numerous biological and medical applications, as well as the relative rate of polymerization as compared to the heat transfer rate. Additionally, the maximum functional group conversion is an important parameter and is a strong function of the initiation conditions, decreasing from 96% (1 wt.-% DMPA, $I_0 = 150$ mW/cm²) to 94% (1 wt.-% DMPA, $I_0 = 5$ mW/cm²) to 86% (0.1 wt.-% DMPA, $I_0 = 150$ mW/cm²) to 62% (0.1 wt.-% DMPA, $I_0 = 5$ mW/cm²). The severe restrictions on the mobility of the reacting species in these highly crosslinked anhydride networks lead to the trapping of radicals, pools of unreacted monomers, unreacted pendant functional groups, and a maximum attainable double bond conversion.

If equal reactivity of the double bonds is assumed, then the conversion of monomer, X_m , is given by

$$X_m = 1 - (1 - P)^2 \quad (1)$$

where P is the total double bond conversion. Thus, for the range of initiation rates reported here, 0.2–14.4% of unreacted monomer (i.e., monomer with neither double bonds reacted) will be present at the highest and lowest double bond conversions, respectively. Unreacted monomer can plasticize the final networks, rendering them more pliable and decreasing mechanical properties. In addition, unreacted monomer may diffuse from the network or be released upon degradation, which will have important implications when assessing the biocompatibility of these highly crosslinked polyanhydride networks.

Photopolymerizing Thick Constructs

Many biological and medical applications for in situ forming degradable biomaterials require facile fabrication of complex-shaped, thick objects (e.g., filling a bone or cartilage defect). However, while photoinitiated polymerizations of multifunctional monomers are widely employed in applications for the production of thin films, photopolymerizing thick polymer samples can be quite challenging. By design, photoinitiator molecules strongly absorb the initiating light, thereby leading to dramatic light attenuation in thick monomer layers. Light attenuation leads to a gradient in the initiation rate; slower polymerization rates in regions farther from the light source; a temperature gradient generated by a slower heat transfer rate in comparison to the rate of heat generated from the exothermic polymerization; and in extreme cases, no polymerization beyond a certain critical depth where the effective light intensity approaches zero.

One approach to address problems associated with the depth of polymerization is to use photobleaching initiators.^[33] These systems allow deeper penetration of the polymerizing light as the absorbance of the initiator decreases with exposure time (i.e., a self-eliminating light-gradient is present). One such initiator system that photobleaches is camphorquinone (CQ) with an amine reducing agent (e.g., ethyl-4-*N,N*-dimethylaminobenzoate, 4EDMAB). The photobleaching effect of CQ is shown in Figure 4, along with the conversion profile as a function of time and depth for the polymerization of a thin film; a thicker sample polymerized under the same conditions; and a 1 mm thick sample polymerized with DMPA and UV light. At 1 mm depth in the DMPA initiated sample, the maximum conversion achieved is about 10% due to light attenuation in the sample. At 4 mm depth in the CQ initiated sample, however, a conversion is reached that is similar to that achieved at the surface (90%). Thus the photobleaching initiator system circumvents problems associated with light attenuation allowing photopolymerization of thicker samples.

Temporal Control of the Polymerization

Photopolymerization of multifunctional monomers has additional advantages besides fast reaction rates at ambi-

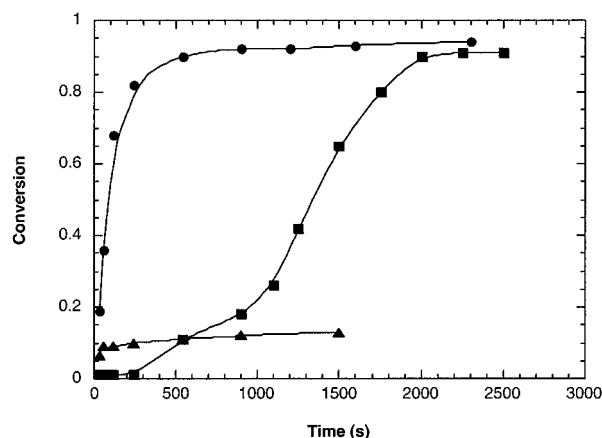


Figure 4. Double bond conversion as a function of time for the polymerization of MSA: as a thin film using 2.0 wt.-% CQ, 1.0 wt.-% 4EDMAB, 200 mW/cm² of 470–490 nm light (●), at a depth of 4 mm using 2.0 wt.-% CQ, 1.0 wt.-% 4EDMAB, 200 mW/cm² of 470–490 nm light (■), and at a depth of 1 mm using 1.0 wt.-% DMPA and 5 mW/cm² of 365 nm light (▲).

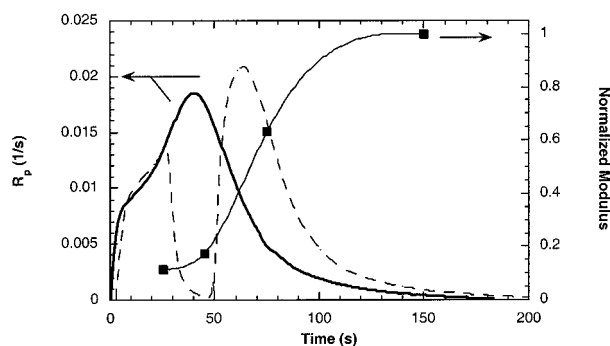


Figure 5. Polymerization rate and modulus as a function of time during the polymerization of MSA polymerized with a constant rate of initiation (—) and a temporally varying rate of initiation (---). Modulus is shown for the sample polymerized with uniform initiation.

ent temperatures, and these include spatial and temporal control of the photoinitiation process. Specifically, the polymerization can be turned on and off by simply shuttering the initiating light source.^[34] Figure 5 illustrates the facile control of the polymerization rate by comparing the polymerization of MSA by continuous exposure to the polymerization of MSA that is intermittently exposed to the light source. Specifically, the system was polymerized for 30 s, left in the dark for 20 s, and then re-exposed until complete polymerization. Note that the rate of polymerization rapidly drops to zero when the light source is shuttered and initiation is ceased. Such temporal control is not readily achieved in thermally and redox initiated polymerization, and is a particularly useful aspect of photoinitiated polymerizations. The inability to control and stop polymerization can be particularly deleterious for in situ forming biomaterials. For example, many current problems with methyl methacrylate based bone

cements relate to lack of control of the initiation and polymerization process, which leads to thermal run-away and tissue necrosis.

In addition to temporal control of the polymerization rate, the polymerizing system is undergoing dramatic changes in mechanical properties during this time frame (from a liquid to a loosely crosslinked rubbery gel to a highly crosslinked glassy network), as observed in the normalized tensile modulus data. Hence, the polymerization can be stopped to coincide with desirable material properties. For example, a partially polymerized, rubbery gel can be contoured or wrapped around an object and then subsequently exposed to the initiating light to form the final rigid product. Several applications that take advantage of this temporal control of the polymerization can be envisioned, one example being a contourable fracture fixation plate.

Degradation Behavior of Highly Crosslinked Anhydride Networks

The cumulative degradation behavior of several different crosslinked polyanhydrides is shown in Figure 6.^[35] The degradation rate of these disks ($D = 16$ mm, $t = 1.8$ mm) was followed at 37°C in PBS buffer at pH 7.4, and the mass loss data follow linear profiles, which are characteristic of a surface erosion mechanism. The hydrophobic backbone of the multifunctional monomer along with the high crosslinking density of the final polymer network prevents water transport throughout the bulk of the material, so only the anhydride linkages at or near the surface of the polymer hydrolyze. In addition to confining degradation of the anhydride linkages to the polymer surface, the rate of degradation is controlled mainly by the hydrophobicity of the network, which is readily altered through changes in the monomer chemistry and/or the incorporation of inert species (e.g., linear polymers) of varying hydrophobicity. For example, the degradation behavior of two homopolymer networks synthesized from MSA and MCPH is shown in Figure 6. The poly(MSA) networks degrade at a rate of 3.4×10^{-2} mm/h, and this disk was completely degraded in 50 h. In contrast, the more hydrophobic poly(MCPH) networks degrade approximately two orders of magnitude slower than the poly(MSA) networks at a rate of 1.9×10^{-4} mm/h. If one assumes that surface erosion is maintained throughout degradation of the entire disk, then this sample would take nearly 12 months to completely erode. As anticipated, copolymerization of the two monomers allows one to vary the degradation rate and span time scales from 2 d to 1 year. For example, a 25:75 poly(MSA:MCPH) disk erodes at a rate of 3.8×10^{-4} mm/h. An alternative strategy to alter the degradation kinetics is to create semi-interpenetrating polymer networks (semi-IPNs). Semi-IPNs can provide many advantages including: reducing the concentration of reactive groups, thereby minimizing the polymeriza-

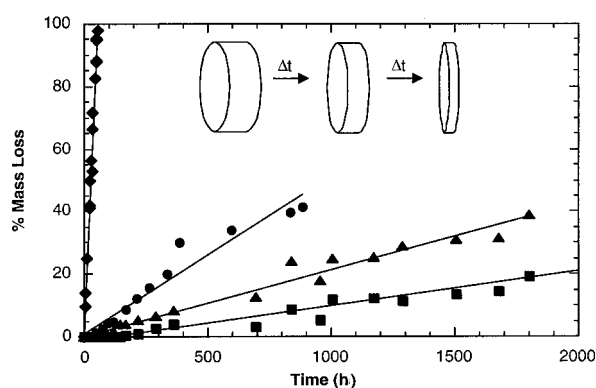


Figure 6. Cumulative percent mass loss as a function of degradation time for poly(MSA) (\blacklozenge), semi-IPN composed of 50 wt.-% crosslinked MSA and 50 wt.-% linear poly(CPP:CPH) (\bullet), 25:75 poly(MSA:MCPH) (\blacktriangle), and poly(MCPH) (\blacksquare).

tion exotherm and volume shrinkage, and altering many macroscopic properties of the network, especially the mechanical properties. Figure 6 shows the degradation behavior of a semi-IPN synthesized by photopolymerizing the MSA monomer in the presence of a linear copolymer of CPP and CPH. The final disk was comprised of 50 wt.-% MSA and 50 wt.-% poly(CPP:CPH), and compared to the poly(MSA) homopolymer, this disk eroded 40 times more slowly.

Fabricating Multi-Laminated Devices

Photopolymerization of multifunctional monomers provides a facile way to produce multi-laminated network structures where each layer can contribute a unique property or feature to the overall device.^[36] For example, each layer can contain a polymer with different mechanics, swelling capacities, degradation rates, and doped with different compounds at varying concentrations. Here, we illustrate how methacrylated anhydride monomers can be used to create a multi-laminated device with programmable drug release behavior. Specifically, a four-layer matrix device was prepared where each alternating layer was loaded with a model drug compound (rhodamine B base, RBB). The device was synthesized in a four-step process, whereby each layer (with or without RBB) was photopolymerized sequentially one on top of the next. As shown in Figure 7, the drug release rate profile exhibits a pulsatile release pattern; where the zero release rate segments represent the lack of any drug release during the erosion of the first and third drug-free layers, and the constant-rate drug release corresponds to the surface erosion of the second and fourth drug-loaded layers. The corresponding cumulative drug release exhibits stepwise changes; the linear increase in the segments represents a constant-rate drug release, and the flat segments represent the absence of any drug release. Since the release rate is directly proportional to the drug loading, one can program any desired release rate by immobilizing suitable

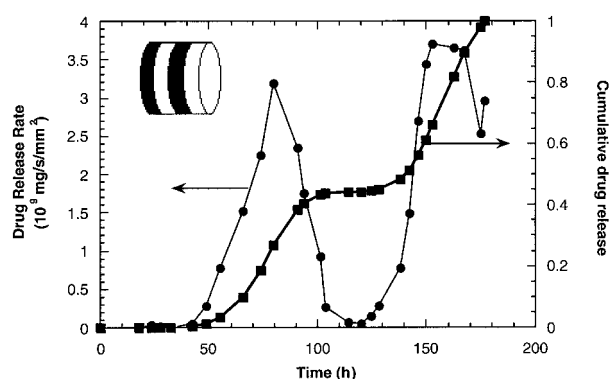


Figure 7. Drug release rate (—●—) and cumulative drug release (—■—) in PBS buffer at 25 °C as a function of degradation time for a four-layer laminated structure of poly(MSA) containing alternating layers loaded with rhodamine B base.

drug concentrations in each constituent layer, or the drug release can be switched from one type to another by loading different types of drugs in each layer.

The spatial control of photopolymerization along with the ability to build-up complex structures through a layer-by-layer photolamination technique also allows the rapid production of complex 3-dimensional objects. Figure 8 compares a human knee X-ray^[37] to a prototype distal end of a human femur created from a data set from the Visible Human Project using a dynamic mask generating stereolithography technique.^[38]

Kinetic Chain Lengths in Highly Crosslinked Networks: Analysis of Degradation Products

While the application of these degradable and photocross-linkable multifunctional anhydride monomers is quite diverse and exciting, the materials can be further utilized from a fundamental perspective to provide insight into the polymerization behavior of multifunctional monomers. In particular, since these dimethacrylated monomers react to form highly crosslinked networks with hydrolyzable anhydride crosslinks, the degradation products can be analyzed to provide valuable information regarding the distribution of kinetic chain lengths in highly crosslinked networks. For multifunctional monomer systems, this information was previously unavailable because of the insolubility of the evolving network structure, but knowledge of the kinetic chain lengths provides a great deal of insight related to initiation, propagation, and termination mechanisms (especially as a function of conversion). In addition, this information has practical importance as many medical applications of degradable materials require that the molecular weight of the degradation products remain below a critical threshold of 40 000 Da below which the body can easily process.^[39]

Figure 9 shows a typical MALDI-TOF spectrum (inset) of the poly(methacrylic acid) degradation products from a highly crosslinked network synthesized from MSA.^[40]

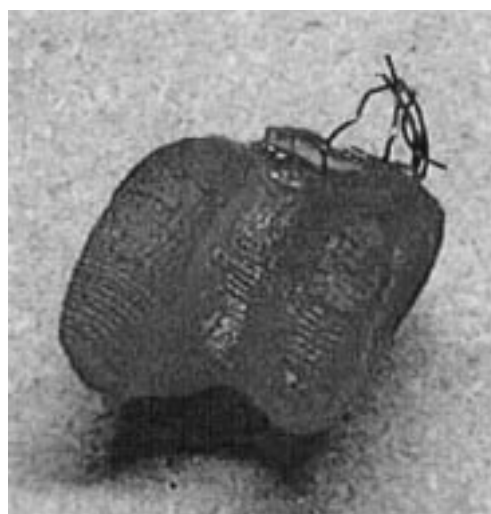


Figure 8. Top: A polymer prototype of the distal end of a human femur recreated using data from the Visible Human Project and a dynamic mask generating stereolithography technique involving photopolymerization.^[38] Bottom: X-ray adapted from Michael L. Richardson, MD.^[37]

The monomeric repeat unit is clearly resolved, and the spectrum visibly extends from chains with 5 to 24 repeat units. In addition, the distribution of kinetic chain lengths was examined as a function of conversion. Specifically, one system was reacted to 40% conversion, and a second system was reacted to 80% conversion. The two networks were degraded and their degradation products analyzed. The number fraction of n -mers, N_n , was plotted as a function of the number of monomeric repeat units in the kinetic chain, n . Due to the noise in the spectra at high molecular weights, the tails of the degradation products were fit exponentially to extrapolate the number fraction of high molecular weight chains. The solid lines represent

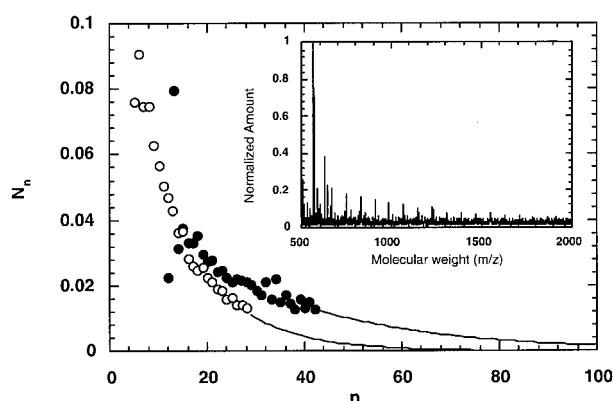


Figure 9. MALDI-TOF data for the distribution of the number of n -mers, N_n , as a function of chain size n for oligo(MSA) photopolymerized with 10 (\bullet) and 100 (\circ) mW/cm^2 of ultraviolet light.

the fitted data. In these experiments, the collected data are a cumulative distribution of all the kinetic chains formed to that point in the polymerization.

Several features are important to note in the distributions of the kinetic chain lengths with conversion. The MSA network that was polymerized to high conversion had a distribution that was shifted to significantly lower molecular weights compared to the system that was polymerized to low conversion. Specifically, the number-average kinetic chain lengths (n_n) were 17 and 37 for the networks reacted to 80% and 40% conversion, respectively. These results are indicative of the diffusion limitations on the propagating species at higher conversion, which contributes to trapping of radicals and to shorter kinetic chain lengths for those chains initiated later in the polymerization. In addition, the polydispersity, Q , was 1.28 in the low conversion network and 1.50 in the high conversion network. The broadening of the kinetic chain length distribution supports the hypothesis of diffusion limitations that chains initiated at low conversions will have higher molecular weights compared to chains initiated at higher conversion. Using multifunctional monomers of varying functionality, size, and stiffness, systematic studies of the kinetic chain length distributions coupled with detailed kinetic data should provide a great deal of insight into the complex reactions of multifunctional monomers.

Potential Applications

We are particularly interested in exploring the use of multifunctional anhydride monomers for numerous orthopedic biomaterial applications. For example, when combined with a photoinitiated polymerization mechanism, these materials can be reacted in situ to form high strength and surface eroding polymers. One might envision future applications where a complex bone defect is filled with a multifunctional anhydride monomer mixed with a hydroxyapatite (i.e., the mineral phase of bone) fil-

ler and photopolymerized to form a composite structure, in a manner similar to filling caries with tooth-colored dental restorations. In contrast to dental restorations, however, the final high strength network would erode away in a controlled fashion to match the rate of bone healing. In addition, temporal control of the polymerization would allow fabrication of contourable fracture fixation plates. Since the networks degrade, antibiotics to prevent infections or bone morphogenic proteins to accelerate bone regrowth can be added to the matrix and released at a rate controlled by degradation. Surface eroding networks can provide many advantages for numerous drug delivery applications,^[41–44] as the release time and rate are directly related to the polymer erosion and device geometry. Furthermore, advanced stereolithographic techniques can be used to photopolymerize complex, three-dimensional architectures with these multifunctional monomers that may provide benefits for applications related to tissue engineering.

Acknowledgement: The authors thank numerous collaborators for technical contributions to this manuscript including Amy Burkoth, Dina Svaldi-Muggli, Jennifer Young, Sanxiu Lu, and Jason Burdick. In addition, we thank the National Science Foundation (BES-9734236), the National Institutes of Health (AR44375), and the Packard Foundation for financial support of this research.

Received: September 1, 2000

Revised: January 11, 2001

- [1] K.S. Anseth, S. M. Newman, C. N. Bowman, *Adv. Polym. Sci.* **1995**, 122, 177.
- [2] J. G. Kloosterboer, *Adv. Polym. Sci.* **1988**, 84, 1.
- [3] L. J. Mathias, S. H. Kusefoglu, A. O. Kress, S. Lee, J. R. Wright, D. A. Culberson, S. C. Warren, R. M. Warren, S. Huang, D. R. Lopez, J. E. Ingram, C. W. Dickerson, M. Jenó, R. J. Halley, R. F. Colletti, G. Cei, C. C. Geiger, *Makromol. Chem., Macromol. Symp.* **1991**, 51, 153.
- [4] A. R. Kannurpatti, R. W. Peiffer, C. A. Guymon, C. N. Bowman, in: "Polymers in Optics: Physics, Chemistry, and Applications", R. A. Lessard, W.F. Frank, Eds., SPIE-International Society for Optical Engineering, Bellingham 1996, p. 136.
- [5] J. G. Kloosterboer, G. F. C. M. Lijten, *ACS Symp. Ser.* **1988**, 367, 409.
- [6] P. Allen, G. Simon, D. Williams, E. Williams, *Macromolecules* **1989**, 22, 809.
- [7] W. D. Cook, *Polymer* **1992**, 33, 2152.
- [8] K. S. Anseth, C. M. Wang, C. N. Bowman, *Polymer* **1994**, 35, 3243.
- [9] S. Zhu, Y. Tian, A. E. Hamielec, Eaton DR, *Macromolecules* **1990**, 23, 1144.
- [10] D. Li, S. Zhu, A. E. Hamielec, *Polymer* **1993**, 34, 1383.
- [11] J. E. Moore, in: "Chemistry and Properties of Crosslinked Polymers", S. S. Labana, Ed., Academic Press, San Diego 1977, p. 535.

- [12] J. G. Kloosterboer, G. F. C. M. Lijten, H. Boots, *Makromol. Chem., Macromol. Symp.* **1989**, *24*, 223.
- [13] J. E. Elliot, C. N. Bowman, *Macromolecules* **1999**, *32*, 8621.
- [14] D. T. Landin, C. W. Macosko, *Macromolecules* **1988**, *21*, 846.
- [15] E. Selli, I. R. Bellobono, in: "Radiation Curing in Polymer and Technology", J. P. Fouassier, J. F. Rabek, Eds., Elsevier Science, New York 1993, vol. 3, chap. 1.
- [16] K. S. Anseth, C. N. Bowman, *J. Polym. Sci., Part B: Polym. Phys.* **1995**, *33*, 1769.
- [17] A. R. Kannurpatti, J. W. Anseth, C. N. Bowman, *Polymer* **1998**, *39*, 2507.
- [18] C. N. Bowman, N. A. Peppas, *Macromolecules* **1991**, *24*, 1914.
- [19] C. Decker, *Polym. Int.* **1998**, *45*, 133.
- [20] A. Matsumoto, *Adv. Polym. Sci.* **1995**, *123*, 41.
- [21] K. S. Anseth, C. Decker, C. N. Bowman, *Macromolecules* **1995**, *28*, 4040.
- [22] E. W. Nelson, A.B. Scranton, *J. Polym. Sci., Polym. Chem.* **1996**, *34*, 403.
- [23] J. Hill-West, S. Chowdhury, A.S. Sawhney, C. P. Pathak, R. Dunn, J. A. Hubbell, *Obstet. Gynecol.* **1994**, *83*, 59.
- [24] A. S. Sawhney, C. P. Pathak, J. A. Hubbell, *Macromolecules* **1993**, *26*, 581.
- [25] J. A. Hubbell, *Curr. Opin. Biotech.* **1999**, *10*, 123.
- [26] D. K. Han, K. D. Park, J. A. Hubbell, Y. H. Kim, *J. Biomat. Sci.-Polym. E.* **1998**, *9*, 667.
- [27] K. S. Anseth, V. R. Shastri, R. Langer, *Nature Biotechnology* **1999**, *17*, 156.
- [28] D. C. Svaldi-Muggli, M. S. thesis, Department of Chemical Engineering, University of Colorado, 1997.
- [29] J. S. Young, K. D. Gonzales, K. S. Anseth, *Biomaterials* **2000**, *21*, 1181.
- [30] K. S. Anseth, L. M. Kline, T. A. Walker, K. J. Anderson, C. N. Bowman, *Macromolecules* **1995**, *28*, 2491.
- [31] K. S. Anseth, C. M. Wang, C. N. Bowman, *Macromolecules* **1994**, *27*, 650.
- [32] D. S. Muggli, A. K. Burkoth, S. A. Keyser, H. R. Lee, K. S. Anseth, *Macromolecules* **1998**, *31*, 4120.
- [33] J. A. Burdick, A. J. Peterson, K. S. Anseth, *Biomaterials*, in press.
- [34] A. K. Burkoth, K. S. Anseth, *ACS Symp. Ser. – Biorelated Polymers*, in press.
- [35] D. S. Muggli, A. K. Burkoth, K. S. Anseth, *J. Biomed. Mater. Res.* **1999**, *46*, 271.
- [36] S. Lu, Ph.D. thesis, Department of Chemical Engineering, University of Colorado 1999.
- [37] X-ray adapted from website: www.scar.rad.washington.edu/RadAnat/KneeAP.html, © Michael L. Richardson, MD, 1997.
- [38] J. S. Young, S. T. Fox, K. S. Anseth, *J. Manufac. Sci. Eng.* **1999**, *121*, 474.
- [39] V. Hofmann, H. Ringsdorf, E. Schaumloffel, *Makromol. Chem.* **1979**, *180*, 595.
- [40] A. K. Burkoth, K. S. Anseth, *Macromolecules* **1999**, *32*, 1438.
- [41] K. Leong, B. Brott, R. Langer, *J. Biomed. Mater. Res.* **1985**, *19*, 941.
- [42] U.S. 4,789,724 (1988), invs: A. Domb, R. Langer.
- [43] A. Domb, S. Amselem, J. Shah, M. Maniar, *Adv. Polym. Sci.* **1991**, *107*, 93.
- [44] H. Brem, S. Piantodosi, P. C. Burger, M. Walker, R. Selker, N. A. Vick, K. Black, M. Sisti, S. Brem, G. Mohr, P. Muller, R. Morawetz, S. C. Schold, *Lancet* **1995**, *345*, 1008.